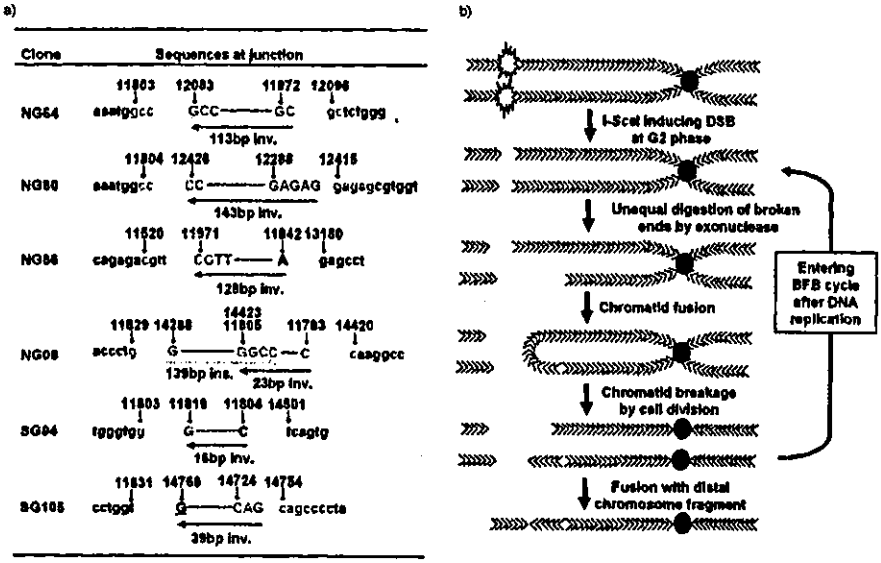

Fig. 5. Complicated DNA rearrangements in thymidine kinase (TK)-deficient mutants from TSCE5 cells. **a:** DNA sequences of the junctions of six mutants with complicated DNA rearrangements (Fig. 4). Sequences with small letters are outside of the junction. Blue-left arrows and green-right arrows show inverted and right directed sequences in parts of deleted region, respectively. Sequences indicated by red capitals indicate the microhomology at junctions. **b:** A model for mechanisms eliciting the complicated DNA rearrangements produced by double-strand breaks (DSBs). Two broken ends of DSBs on sister chromatids in G_2 phase cells are unequally processed by exonuclease, and fuse to each other to form a chromatid bridge. The dicentric chromatid is torn by cell division, producing daughter cells with broken chromosomes, which fuse with telomeric chromosome fragments. Some broken chromosomes enter a breakage-fusion-bridge (BFB) cycle, leading to more complicated rearrangements with inverted and right directed sequences at the junction.

[Haber, 2000; Jackson, 2002]. Interestingly, six other mutants exhibited complicated DNA rearrangements that involved a deletion combined with an inverted sequence that was part of the deleted sequence (Fig. 5a). Clone NG08 exhibited a particularly complicated rearrangement consisting of an inverted sequence and a forward sequence. Because these inverted sequences also joined through a 0- to 5-bp microhomology, EJ probably contributed to the rearrangement. We also examined these rearranged mutants by SKY analysis. There was, however, no apparent alteration in chromosome 17q and no translocated chromosome fragments derived from chromosome 17 in the mutants (data not shown).

HR Always Resulted in Non-Crossing-Over Gene Conversion

We also analyzed 38 TSCER2 revertants. Every revertant showed LOH at the I-*Sce*I site accompanied by an increased band intensity of the intact allele (Fig. 1b). This means that HR between homologous chromosomes produced the revertants, as expected, resulting in homozygous LOH. Extended LOH analysis revealed that no revertant showed LOH at any polymorphic marker surrounding the *TK* gene (Fig. 3). Every LOH was limited to the *TK* gene, implying that these revertants were the result of gene conversion without crossing-over. The tract length of the gene conversion varied in the revertants. At least 14 (37%) of the revertants were generated by >876-bp tract gene conversion.

No Small Deletions or Small Tract Gene Conversions Were Observed in Nonselected Cells

After transfecting TECS5 cells with the I-*Sce*I expression vector pCMV3xnls-I-*Sce*I, we isolated a total of 1,442 independent clones without TFT selection and analyzed their I-*Sce*I sites by PCR. All clones except one had the intact I-*Sce*I site and were identical to parental TSCE5 cells. The exceptional clone, however, had a deletion of >1 kb that included exons 5 and 6 (data not shown).

DISCUSSION

Contribution of EJ and HR for Repairing a Chromosome DSB

The assay system we established in the present study can trace the fate of a DSB in the human genome. We succeeded in integrating an I-*Sce*I site into an endogenous single-copy gene by two gene-targeting steps to minimize the introduction of other exogenous DNA sequences. It is likely that the DSB generated at the I-*Sce*I site was similar to DSBs

induced by low-dose irradiation in an intact genomic region, and the fate of the DSB seemed to depend on the physiological response to the exogenous DNA damage. The I-*Sce*I induced DSBs in G_1 phase were chromosomal breaks, while during late S and G_2 phases they were single or double chromatid breaks. EJ can operate throughout the cell cycle but may be more important during G_1 phase, while HR is a post-DNA-replication repair pathway [Johnson and Jasin, 2000; Hendrickson, 1997]. HR likely repairs chromatid breaks occurring in the late S and G_2 phases, and for chromosomal breaks that escape from EJ in the G_1 phase and turn into sister-chromatid breaks after DNA replication. Breaks on both sister chromatids can be repaired only by inter-allelic HR, although either chromatid break could be effectively repaired by sister-chromatid HR, which can not be demonstrated in our system [van Gent et al., 2001]. Because the human lymphoblastoid cells used in this study were unsynchronized and more than 50% were in G_1 phase [Little et al., 1995], the genetic consequences of DSB repair in the present system are mainly a reflection of chromosomal DSBs.

By transfecting the I-*Sce*I expression vector into the cells, TK-deficient mutants from TSCE5 cells and TK-proficient revertants from TSCER2 cells were recovered 130- and 200-fold more frequently than spontaneous mutants, respectively, suggesting that DSBs can stimulate inter-allelic HR as well as EJ. Because the revertant frequency was much less than the mutant frequency, however, almost all DSBs appear to be repaired by EJ. The relative contribution of EJ and HR for repairing DSBs in mammalian cells varies in the cells and the systems used to detect them, but EJ is the predominant mechanism for DSB repair in most cases [Takata et al., 1998; Essers et al., 2000]. Liang et al. [1998] and Johnson and Jasin [2000] demonstrated that approximately 30–50% of DSBs generated at an I-*Sce*I site in tandem repeated recombination substrates were repaired by HR, with the rest repaired by EJ. The system is, however, strongly biased in favor of detecting intra-chromosomal recombination between the repeated sequences. Almost 1% of DSBs in LINE-1 sequences (a repetitive element found throughout the mammalian genome at approximately 1×10^5 copies) was repaired by HR [Tremblay et al., 2000]. The contribution of HR for repairing chromosomal DSBs in a single copy mammalian gene must be quite low, however, because only the homologous allele is available as a recombination partner. Recently, Stark and Jasin [2003] estimated that an I-*Sce*I-induced DSB in a single-copy gene in mouse ES cells is repaired at least 1,000-fold more efficiently by EJ than by inter-allelic HR. Our present study strongly supported their estimation; nearly 100% of chromosomal DSBs were repaired by EJ in human TK6 cells, and HR rarely contributed to the repair.

The assay system described in the present study cannot recover every genetic consequence of EJ and HR. Because the I-*Sce*I site is inserted in intron 4 of the functional *TK* allele, in a position 75 bp upstream of exon 5, a small deletion caused by EJ that does not affect the TK function will not be recovered as a TFT-resistant mutant. Similarly, a small-tract gene conversion not extending to the point mutation in exon 5 (base 23 of exon 5) also will not be rescued in the reversion assay (Fig. 1a). If small deletions and small-tract gene conversions are the major products of EJ and HR, respectively, the mutants and revertants recovered in this assay system may not accurately reflect DSB repair. In fact, Lin et al. [1999] reported that I-*Sce*I induced DSBs in mouse chromosomes were mainly repaired by EJ, resulting in very few nucleotide deletions. To clarify this issue, we isolated 1,442 independent clones from TSCE5 cells without drug selection after transfection with the I-*Sce*I expression vector and examined their I-*Sce*I site. No small deletions or small-tract gene conversions were observed; the one mutant clone detected had a 1-kb deletion, which should have been detected as a TK-deficient mutant. Although the efficiency of inducing DSBs by transfection of the I-*Sce*I expressing vector is not clear and the number of analyzed clones may not be sufficient, this result would indicate that our assay system detected most of the genetic consequences resulting from the repair of DSBs and was not strongly biased in favor of specific genetic events.

Genetic Consequences of Chromosomal DSBs Repaired by EJ

Around 70% (16/22) of the small deletions we analyzed by PCR and sequencing exhibited simple deletions ranging from 109 to 3,964 bp with a 0- to 6-bp microhomology at the junction of the deletion. These deletions can be explained by an NHEJ model, which is a general EJ mechanism found in mammalian cells as well as in other species [Haber, 2000; Jackson, 2002]. Single-strand annealing (SSA), which is a special form of HR that works efficiently on repeated sequences flanking DSBs in yeast and mammalian cells [Paques and Haber, 1999; Lin et al., 1990], can cause simple deletions in a nonconservative manner. This mechanism can be excluded for generating the deletions, however, because it would need at least a 30-bp homology at the sequence junctions [Sugawara et al., 2000]. SSA may not function for DSB repair in a single-copy gene, but it may have been responsible for some of the unanalyzed large deletions. In contrast, six other mutants exhibited complicated DNA rearrangements in which a deletion was combined with an inverted sequence that was part of the deleted sequence (Fig. 5a). Because these inverted sequences also joined through 1- to 5-bp microhomologies, EJ probably contributed to the rearrangements. We speculate that some DSBs occurring in late S or G_2 phase could lead to the rearrangements (Fig. 5b). DSBs induced by I-*Sce*I expression occur at the same position on both sister chromatids after DNA replication. The ends of the broken sister chromatids that are unequally processed by exonuclease may

occasionally fuse to each other to form a chromatid bridge. A dicentric chromatid torn by cell division produces daughter cells with broken chromosomes, and the telomeric chromosome fragment may fuse again. Clone NG08 exhibited a more complicated rearrangement consisting of an inverted sequence and a forward sequence, implying that a breakage-fusion-bridge (BFB) cycle occurred. A BFB cycle resulting from telomere loss is associated with chromosome instability and sometimes results in high-copy gene amplification or nonreciprocal translocation, which is commonly observed in tumor cells [Kuo et al., 1994; Coquelle et al., 1997]. These specific DNA rearrangements, however, may be observed in I-*Sce*I-induced mutagenesis at a high frequency because of the simultaneous occurrence of DSBs at the same position on both sister chromatids. In spite of the complex DNA rearrangement, these mutants did not reveal any gross changes in chromosome 17q. Lo et al. [2002] and Pipiras et al. [1998] reported that DSBs induced by I-*Sce*I cause chromosomal instability, and sometimes result in large interstitial deletions and intra-chromosomal amplifications through a BFB cycle. Other unanalyzed mutants from TSCE5 in this study, which are expected to have deletions of ≥5 kb, may show gross structural changes initiated by a BFB cycle, although they would be a minor consequence of DSBs.

Genetic Consequences of Chromosomal DSBs Repaired by HR

In the HR repair model, recombinational intermediates (Holliday junctions) may be resolved as a reciprocal exchange (crossing-over) or a nonreciprocal transfer of genetic information (gene conversion without crossing-over) [Szostak et al., 1983]. Both products appear equally for meiotic recombination at some loci [Cromie et al., 2001]. Molecular analysis of 38 revertants from TSCER2 cells, however, clearly demonstrated that gene conversion was preferred for repairing DSBs, because no revertants showed LOH at any of the distal microsatellite markers. HR for repairing DSBs generally occurs during postreplication, and inter-allelic recombination is also thought to occur between chromatids in the late S and G_2 phase. Theoretically, reciprocal exchange can produce revertants that retain distal heterozygosity if the two chomatids involved as recombination partners are co-segregated by cell division. Because co-segregation presumably will occur 50% of the time, resulting in LOH at distal markers, the participation of reciprocal exchange for the generation of these revertants can be excluded. In contrast, most HR products occurring spontaneously or induced by ionizing irradiation in autosomal recessive gene mutation assays in mouse and human cells are the result of reciprocal exchange [Honma et al., 1997b, 2000, 2001]. This may be because of the strong bias for recovery of HR products with crossing-over involving nontargeted mutagenesis; reciprocal exchange that affects a particular target (e.g., the *TK* gene) must occur at relatively a low frequency. Quintana et al. [2001] developed a cell line from TK6 that has a compound heterozygous *TK* gene ($TK^{+/-}$) and examined TK-proficient revertants induced by ionizing irradiation and a chemical mutagen. These investigators also did not recover any revertants with crossing-over, and they estimated that non-crossing-over is approximately 700-fold more frequent than reciprocal exchanges on a yield-per-kilobase basis. A preference for recovery of gene conversion rather than reciprocal exchanges in mitosis also was reported in yeast and mammalian cells [Paques and Haber, 1999; Cromie et al., 2001]. In yeast, however, about 10% of inter-allelic HR events involved crossing-over [Nickoloff et al., 1999], while almost all inter-allelic HR in mammalian cells was of a non-crossing-over type [Stark and Jasin, 2003]. Thus, Holliday intermediates must be resolved with bias, especially in mammalian cells. The strong suppression of reciprocal exchanges may contribute to the maintenance of genomic integrity because reciprocal exchange could bring about large-scale genetic alterations, including translocations [Richardson et al., 1998].

Although the present study showed that the contribution of HR for repairing chromosomal DSBs is quite low, HR must be essential for maintaining genomic integrity in mammalian cells. Knocking out *Rad51* and other genes involved in HR, such as *Rad52*, *Xrcc2*, and *Xrcc3*, is lethal, enhances sensitivity to ionizing irradiation and chemicals, and/or influences the fidelity of HR [Rijkers et al., 1998; Cui et al., 1999; Takata et al., 2001; Sale et al., 2001; Brenneman et al., 2002]. These observations indicate that HR has an important role in overcoming some genetic stresses. Most spontaneous DSBs in mammalian cells is thought to be produced by replication stress rather than exogenous effects [Haber, 1999]. Single-strand breaks are frequently converted during nucleotide and base excision repair to DSBs when replication folks are encountered. These types of DSBs could be repaired efficiently by HR between sister chromatids in the late S and G_2 phases, which would be critical for maintaining genomic integrity as well as cell viability. Thus, HR may be important for repairing chromatid breaks generated by the replication stress [Kadyk and Hartwell, 1992], but not for chromosome breaks. The role of inter-allelic HR remains unclear, although it is clearly induced by DSBs. Inter-allelic HR contributes greatly to genomic instability, in particular LOH in tumorigenesis, and may be associated with genetic and environmental factors [Lasko et al., 1991; Moynahan and Jasin, 1997].

We conclude that almost all chromosomal DSBs are repaired by EJ in human cells, and that when HR is involved, it is in the form of gene conversion without crossing-over. These findings strongly support the preferences of mammalian DSB repair pathways reported previously. The present system established in the present study can trace the fate of DSBs in mammalian cells quantitatively as well as qualitatively, and holds promise for elucidating genetic and

environmental factors that influence DSB repair [Palmer et al., 2003].

ACKNOWLEDGMENTS

The authors thank Dr. Jac A. Nickoloff (University of New Mexico School of Medicine, New Mexico) for providing the I-*Sce*I expression vector, pCMV3xnls-I-*Sce*I. We also thank Dr. Robert H. Heflich (National Center for Toxicological Research, Arkansas) for helpful comments and review of the manuscript.

REFERENCES

Brenneman MA, Wagener BM, Miller CA, Allen C, Nickoloff JA. 2002. XRCC3 controls the fidelity of homologous recombination: roles for XRCC3 in late stages of recombination. Mol Cell 10:387–395.

Coquelle A, Pipiras E, Toledo F, Buttin G, Debatisse M. 1997. Expression of fragile sites triggers intrachromosomal mammalian gene amplification and sets boundaries to early amplicons. Cell 89:215–225.

Cromie GA, Connelly JC, Leach DR. 2001. Recombination at double-strand breaks and DNA ends: conserved mechanisms from phage to humans. Mol Cell 8:1163–1174.

Cui X, Brenneman M, Meyne J, Oshimura M, Goodwin EH, Chen DJ. 1999. The XRCC2 and XRCC3 repair genes are required for chromosome stability in mammalian cells. Mutat Res 434:75–88.

Elliott B, Richardson C, Winderbaum J, Nickoloff JA, Jasin M. 1998. Gene conversion tracts from double-strand break repair in mammalian cells. Mol Cell Biol 18:93–101.

Essers J, van Steeg H, de Wit J, Swagemakers SM, Vermeij M, Hoeijmakers JH, Kanaar R. 2000. Homologous and non-homologous recombination differentially affect DNA damage repair in mice. EMBO J 19:1703–1710.

Giver CR, Grosovsky AJ. 1997. Single and coincident intragenic mutations attributable to gene conversion in a human cell line. Genetics 146:1429–1439.

Grosovsky AJ, Walter BN, Giver CR. 1993. DNA-sequence specificity of mutations at the human thymidine kinase locus. Mutat Res 289: 231–243.

Haber JE. 1995. In vivo biochemistry: physical monitoring of recombination induced by site-specific endonucleases. BioEssays 17:609–620.

Haber JE. 1999. DNA recombination: the replication connection. Trends Biochem Sci 24:271–275.

Haber JE. 2000. Partners and pathways repairing a double-strand break. Trends Genet 16:259–264.

Hendrickson EA. 1997. Cell-cycle regulation of mammalian DNA double-strand-break repair. Am J Hum Genet 61:795–800.

Honma M, Hayashi M, Sofuni T. 1997a. Cytotoxic and mutagenic responses to X-rays and chemical mutagens in normal and p53-mutated human lymphoblastoid cells. Mutat Res 374:89–98.

Honma M, Zhang LS, Hayashi M, Takeshita K, Nakagawa Y, Tanaka N, Sofuni T. 1997b. Illegitimate recombination leading to allelic loss and unbalanced translocation in p53-mutated human lymphoblastoid cells. Mol Cell Biol 17:4774–4781.

Honma M, Momose M, Tanabe H, Sakamoto H, Yu Y, Little JB, Sofuni T, Hayashi M. 2000. Requirement of wild-type p53 protein for maintenance of chromosomal integrity. Mol Carcinog 28:203–214.

Honma M, Momose M, Sakamoto H, Sofuni T, Hayashi M. 2001. Spindle poisons induce allelic loss in mouse lymphoma cells through mitotic non-disjunction. Mutat Res 493:101–114.

Honma M, Tadokoro S, Sakamoto H, Tanabe H, Sugimoto M, Furuichi Y, Satoh T, Sofuni T, Goto M, Hayashi M. 2002. Chromosomal instability in B-lymphoblastoid cell lines from Werner and Bloom syndrome patients. Mutat Res 522:15.

Jackson SP. 2002. Sensing and repairing DNA double-strand breaks. Carcinogenesis 23:687–696.

Jackson SP, Jeggo PA. 1995. DNA double-strand break repair and V(D)J recombination: involvement of DNA-PK. Trends Biochem Sci 20: 412–415.

Johnson RD, Jasin M. 2000. Sister chromatid gene conversion is a prominent double-strand break repair pathway in mammalian cells. EMBO J 19:3398–3407.

Johnson RD, Jasin M. 2001. Double-strand-break-induced homologous recombination in mammalian cells. Biochem Soc Trans 29:196–201.

Kadyk LC, Hartwell LH. 1992. Sister chromatids are preferred over homologs as substrates for recombinational repair in *Saccharomyces cerevisiae*. Genetics 132:387–402.

Khanna KK, Jackson SP. 2001. DNA double-strand breaks: signaling, repair and the cancer connection. Nat Genet 27:247–254.

Kuo MT, Vyas RC, Jiang LX, Hittelman WN. 1994. Chromosome breakage at a major fragile site associated with P- glycoprotein gene amplification in multidrug-resistant CHO cells. Mol Cell Biol 14: 5202–5211.

Lasko D, Cavenee W, Nordenskjold M. 1991. Loss of constitutional heterozygosity in human cancer. Annu Rev Genet 25:281–314.

Liang F, Han M, Romanienko PJ, Jasin M. 1998. Homology-directed repair is a major double-strand break repair pathway in mammalian cells. Proc Natl Acad Sci USA 95:5172–5177.

Liber HL, Thilly WG. 1982. Mutation assay at the thymidine kinase locus in diploid human lymphoblasts. Mutat Res 94:467–485.

Lin FL, Sperle K, Sternberg N. 1990. Intermolecular recombination between DNAs introduced into mouse L cells is mediated by a nonconservative pathway that leads to crossover products. Mol Cell Biol 10:103–112.

Lin Y, Lukacsovich T, Waldman AS. 1999. Multiple pathways for repair of DNA double-strand breaks in mammalian chromosomes. Mol Cell Biol 19:8353–8360.

Little JB, Nagasawa H, Keng PC, Yu Y, Li CY. 1995. Absence of radiation-induced G1 arrest in two closely related human lymphoblast cell lines that differ in p53 status. J Biol Chem 270:11033–11036.

Lo AW, Sprung CN, Fouladi B, Pedram M, Sabatier L, Ricoul M, Reynolds GE, Murnane JP. 2002. Chromosome instability as a result of double-strand breaks near telomeres in mouse embryonic stem cells. Mol Cell Biol 22:4836–4850.

Moynahan ME, Jasin M. 1997. Loss of heterozygosity induced by a chromosomal double-strand break. Proc Natl Acad Sci USA 94: 8988–8993.

Nickoloff JA, Sweetser DB, Clikeman JA, Khalsa GJ, Wheeler SL. 1999. Multiple heterologies increase mitotic double-strand break-induced allelic gene conversion tract lengths in yeast. Genetics 153:665–679.

Palmer S, Schildkraut E, Lazarin R, Nguyen J, Nickoloff JA. 2003. Gene conversion tracts in *Saccharomyces cerevisiae* can be extremely short and highly directional. Nucleic Acids Res 31:1164–1173.

Paques F, Haber JE. 1999. Multiple pathways of recombination induced by double-strand breaks in *Saccharomyces cerevisiae*. Microbiol Mol Biol Rev 63:349–404.

Pipiras E, Coquelle A, Bieth A, Debatisse M. 1998. Interstitial deletions and intrachromosomal amplification initiated from a double-strand break targeted to a mammalian chromosome. EMBO J 17:325–333.

Quintana PJ, Neuwirth EA, Grosovsky AJ. 2001. Interchromosomal gene conversion at an endogenous human cell locus. Genetics 158:757–767.

Richardson C, Moynahan ME, Jasin M. 1998. Double-strand break repair

by interchromosomal recombination: suppression of chromosomal translocations. Genes Dev 12:3831–3842.

Rijkers T, Van Den OJ, Morolli B, Rolink AG, Baarends WM, Van Sloun PP, Lohman PH, Pastink A. 1998. Targeted inactivation of mouse RAD52 reduces homologous recombination but not resistance to ionizing radiation. Mol Cell Biol 18:6423–6429.

Sale JE, Calandrini DM, Takata M, Takeda S, Neuberger MS. 2001. Ablation of XRCC2/3 transforms immunoglobulin V gene conversion into somatic hypermutation. Nature 412:921–926.

Sargent RG, Brenneman MA, Wilson JH. 1997. Repair of site-specific double-strand breaks in a mammalian chromosome by homologous and illegitimate recombination. Mol Cell Biol 17:267–277.

Stark JM, Jasin M. 2003. Extensive loss of heterozygosity is suppressed during homologous repair of chromosomal breaks. Mol Cell Biol 23:733–743.

Sugawara N, Ira G, Haber JE. 2000. DNA length dependence of the single-strand annealing pathway and the role of *Saccharomyces cerevisiae* RAD59 in double-strand break repair. Mol Cell Biol 20:5300–5309.

Szostak JW, Orr-Weaver TL, Rothstein RJ, Stahl FW. 1983. The double-strand-break repair model for recombination. Cell 33:25–35.

Taghian DG, Nickoloff JA. 1997. Chromosomal double-strand breaks induce gene conversion at high frequency in mammalian cells. Mol Cell Biol 17:6386–6393.

Takata M, Sasaki MS, Sonoda E, Morrison C, Hashimoto M, Utsumi H, Yamaguchi-Iwai Y, Shinohara A, Takeda S. 1998. Homologous recombination and non-homologous end-joining pathways of DNA double-strand break repair have overlapping roles in the maintenance of chromosomal integrity in vertebrate cells. EMBO J 17: 5497–5508.

Takata M, Sasaki MS, Tachiiri S, Fukushima T, Sonoda E, Schild D, Thompson LH, Takeda S. 2001. Chromosome instability and defective recombinational repair in knockout mutants of the five Rad51 paralogs. Mol Cell Biol 21:2858–2866.

Tremblay A, Jasin M, Chartrand P. 2000. A double-strand break in a chromosomal LINE element can be repaired by gene conversion with various endogenous LINE elements in mouse cells. Mol Cell Biol 20:54–60.

Van Dyck E, Stasiak AZ, Stasiak A, West SC. 1999. Binding of double-strand breaks in DNA by human Rad52 protein. Nature 398:728–731.

van Gent DC, Hoeijmakers JH, Kanaar R. 2001. Chromosomal stability and the DNA double-stranded break connection. Nat Rev Genet 2:196–206.

Available online at www.sciencedirect.com
SCIENCE DIRECT®
Mutation Research 539 (2003) 99–108
Genetic Toxicology and Environmental Mutagenesis
www.elsevier.com/locate/gentox
Community address: www.elsevier.com/locate/mutres

Regional mutagenicity of heterocyclic amines in the intestine: mutation analysis of the *cII* gene in lambda/*lacZ* transgenic mice

Toshiaki Itoh[a,b], Tomomi Kuwahara[a], Takayoshi Suzuki[c], Makoto Hayashi[c], Yoshinari Ohnishi[a,*]

[a] *Department of Molecular Bacteriology, Graduate School of Medicine, The University of Tokushima, 3-18-15 Kuramoto-cho, Tokushima 770-8503, Japan*
[b] *Tokushima Research Institute, Otsuka Pharmaceutical Co. Ltd., 463-10 Kagasuno, Kawauchi-cho, Tokushima 771-0192, Japan*
[c] *Division of Genetics and Mutagenesis, National Institute of Health Sciences, 1-18-1 Kamiyoga, Setagaya-ku, Tokyo 158-8501, Japan*

Received 19 August 2002; received in revised form 23 May 2003; accepted 23 May 2003

Abstract

Transgenic mouse assays have revealed that the mouse intestine, despite its resistance to carcinogenesis, is sensitive to the mutagenicity of some heterocyclic amines (HCAs). Little is known, however, about the level and localization of that sensitivity. We assessed the mutagenicity of four orally administered (20 mg/kg per day for 5 days) HCAs—2-amino-1-methyl-6-phenylimidazo[4,5-*b*]pyridine (PhIP) hydrochloride, 2-amino-3-methylimidazo[4,5-*f*]quinoline (IQ), 2-amino-3,4-dimethylimidazo[4,5-*f*]quinoline (MeIQ), and 3-amino-1-methyl-5*H*-pyrido[4,3-*b*]indole (Trp-P-2) acetate—in the intestine of male Muta™Mice. Two weeks after the last administration, we isolated epithelium from the small intestine, cecum, and colon and analyzed *lacZ* and *cII* transgene mutations. PhIP increased the *lacZ* mutant frequency (MF) in all the samples, and in the small intestine, *cII* and *lacZ* MFs were comparable. In the *cII* gene, G:C to T:A and G:C to C:G transversions were characteristic PhIP-induced mutations (which has also been reported for the rat colon, where PhIP is carcinogenic). In the small intestine, PhIP increased the *cII* MF to four-fold that of the control, but IQ, MeIQ, and Trp-P-2 did not have a significant mutagenic effect. In the cecum, *cII* MFs induced by IQ and MeIQ were 1.9 and 2.7 times those in the control, respectively. The MF induced by MeIQ in the colon was 3.1 times the control value. Mutagenic potency was in the order PhIP > MeIQ > IQ; Trp-P-2 did not significantly increase the MF in any tissue. The cecum was the most susceptible organ to HCA mutagenicity.

Subj. Class.: 105650-23-5 (PhIP hydrochloride); 76180-96-6 (IQ); 77094-11-2 (MeIQ); 72254-58-1 (Trp-P-2 acetate)

Keywords: Heterocyclic amine; *lacZ*; Lambda *cII*; Mutant frequency; Intestine

1. Introduction

Spontaneous cancers are common in the human intestine, where there is frequent exposure to dietary mutagens and carcinogens such as the heterocyclic amines (HCAs) found in well-cooked meat. In experimental animals, however, the organ is resistant to the carcinogenic effects of the majority of genotoxic compounds [1]. Although five HCAs—2-amino-6-methyldipyrido[1,2-*a*:3′,2′-*d*]imidazole (Glu-P-1), 2-aminodipyrido[1,2-*a*:3′,2′-*d*]imidazole (Glu-P-2), 2-amino-3-methylimidazo[4,5-*f*]quinoline (IQ), 2-amino-

* Corresponding author. Tel.: +81-88-633-7069; fax: +81-88-633-7069.
E-mail address: ohnishi@basic.med.tokushima-u.ac.jp (Y. Ohnishi).

1383-5718/$ – see front matter © 2003 Elsevier B.V. All rights reserved.
doi:10.1016/S1383-5718(03)00134-7

3,4-dimethylimidazo[4,5-*f*]quinoline (MeIQ), and 2-amino-1-methyl-6-phenylimidazo[4,5-*b*]pyridine (PhIP)—induce intestinal tumors in rats, they have rarely been shown to do so in mice [2,3].

The weak carcinogenicity of HCAs in the mouse intestine is not due to a lack of local mutagenic activity, as has been shown by somatic mutation assays based on endogenous markers and transgenic shuttle vectors [4,5]. Transgenic mouse assays reveal that HCAs increase mutant frequencies (MFs) in the intestines at least as much as they do in the target organs for carcinogenesis. Although PhIP is mutagenic in several organs, it is most potent in the small and large intestine of *lacZ* transgenic Muta™Mice [6] and the colon of *gptΔ* transgenic mice [7]. In female Big Blue® transgenic mice, MeIQ induces *lacI* mutations at a much higher rate in the colon than in the liver and forestomach, which are target organs for carcinogenesis [8]. MeIQx (2-amino-3,8-dimethylimidazo[4,5-*f*]quinoxaline), a hepatocarcinogen, induces *lacI* mutations in the mouse colon as well [9].

We know that the mouse intestine is sensitive to HCAs, but we know little about the level of sensitivity in specific areas. PhIP is mutagenic in both small and large intestine [4–6], but the mutagenic potencies of other HCAs have been reported for only a part of the intestine or not at all.

We used the male Muta™Mouse intestine to study the genotoxic potential of four HCAs—PhIP hydrochloride, IQ, MeIQ, and 3-amino-1-methyl-5*H*-pyrido[4,3-*b*]indole (Trp-P-2) acetate. After the animals were treated, we isolated epithelium from the small intestine, cecum, and colon and extracted the DNA, which we subjected to an in vitro packaging reaction. We assayed lambda shuttle vectors, recovered as viable phages, for *lacZ* and lambda *cII* mutations. We analyzed the frequency and mutational specificity of *cII* mutants induced by PhIP, and showed that PhIP induced the same mutations in the small intestine of mice and the large intestine of rats, despite differences in their susceptibility to carcinogenicity. We compared *cII* MFs induced by HCAs and showed that the epithelium in each intestinal region was distinct in its susceptibility to HCA mutagenesis. The transgenic mouse intestine served as a useful model for the study of genotoxic potency of intestinal carcinogens.

2. Materials and methods

2.1. Chemicals

PhIP hydrochloride, IQ, MeIQ, and Trp-P-2 acetate were purchased from Wako Pure Chemicals (Tokyo). Just before administration, PhIP hydrochloride and Trp-P-2 acetate were dissolved in physiological saline while IQ and MeIQ were dissolved or suspended in corn oil, at a concentration of 2 mg/ml. Phenyl-β-D-galactopyranoside (P-gal) and 5-bromo-4-chloro-3-indolyl-β-D-galactopyranoside (X-gal) were purchased from Sigma Chemical (St. Louis, MO).

2.2. Animals and treatment

Male *lacZ* transgenic mice (Muta™Mouse) with a CDF1 (BALB/c × DBA/2 F1) genetic background were obtained at 4–7 weeks of age from Covance Research Products (Denver, PA). The Muta™Mouse test system carrying integrated lambda gt10 shuttle vectors containing the bacterial *lacZ* gene has been described in detail elsewhere [10]. The mice were housed in plastic cages with hard wood chips for bedding and were fed a standard diet (Oriental MF, Oriental Yeast, Tokyo) and tap water ad libitum. A week before administration of the test compounds, the diet was switched to AIN-76 purified diet (Crea Japan, Tokyo). Administration of the compounds started when the mice were 10 weeks old. The mice in the HCA treatment groups ($n = 5$–7) were fed a HCA daily in a volume of 10 ml/kg body weight for 5 days. The control mice received the same volume of corn oil daily for 5 days. We used the carcinogenic potency database to set the dose of HCA at 20 mg/kg per day [11], which approximates to the TD_{50} values for PhIP, IQ, MeIQ, and Trp-P-2: 28.6, 19.6, 12.3, and 12.6 mg/kg per day, respectively [3].

2.3. Tissue and DNA isolation

Two weeks after the last administration of HCA, the mice were killed by post-caval incision under anesthesia and the intestines were removed. The lumen was flushed with phosphate-buffered saline (PBS), and the intestine was divided into small intestine, cecum, and colon. Each section was cut along the mesenteric line, washed with PBS, quickly frozen

with liquid nitrogen, and stored at −80 °C. Before use, each frozen segment was placed in a plastic dish containing 30 mM EDTA-PBS solution at <4 °C and left to defrost for 30 min. After removing the luminal contents and mesenteric nodes, we placed the segments lumen-side-up in a plastic dish and, with the aid of a microscope, stroked them gently with the back of mosquito forceps to isolate crypt-villus units (sheets) from the mucosal layer. We collected the units in a tube and immediately incubated them with proteinase K solution at 50 °C for 3 h. We extracted DNA as described previously [12]. Without bias (distal or proximal), we cut the colon segment into pieces and randomly partitioned them into two portions. We used one portion (consisting of about two thirds of the total amount of cut pieces) for DNA isolation from the mucosal epithelium and the other portion for DNA isolation from the whole colon.

2.4. lacZ mutation analysis

A 5–10 μl aliquot of DNA solution was removed and used for lambda prophage rescue with a MutaPlax™ packaging extract (Epicentre Technologies, Madison, WI). Screening for *lacZ* mutant phages was carried out by P-gal-based positive selection with *Escherichia coli* strain C (*lac*$^-$*galE*$^-$), and all mutants were confirmed on X-gal plates as previously described [13].

2.5. Lambda cII mutation analysis

We used a MutaPlax *cII*-Select™Kit (Epicentre Technologies) for the lambda *cII* assay. The kit contained lambda packaging extracts and cultures of *hfl*$^+$ *E. coli* strain G1217 for the determination of recovered phage titers and *hfl*$^-$*E. coli* G1225 for the selection of mutant phages. Lambda packaging and positive selection for *cII* mutants was performed according to the manual in the packaging insert, essentially as described by Jakubczak et al. [14] with slight modification. Briefly, 500 μl of the packaged phage solution was incubated with the same volume of strain G1225 cells (OD_{660} = 1.0) at room temperature for 30 min, mixed with 11 ml LB top agar, and plated on four 9 cm dishes containing 6 ml bottom agar. The plates were incubated at 24.5 ± 0.5 °C for 48 h. For titration, a 100 μl aliquot of a 1:100 dilution of the packaged phage was mixed with the same volume of strain G1225 cells and 6 ml LB top agar, plated on two dishes, and incubated at 37 °C for 24 h. Wild-type phage recovered from Muta™Mouse has a *cI*$^-$ phenotype, which permitted plaque formation on the *hfl*$^-$ strain at 37 °C but not at 25 °C. We determined the MF by dividing the number of mutant plaques by the total number of recovered phage titers evaluated from each animal. Generally, we analyzed >2 × 10^5 plaque forming units in each case.

2.6. Sequencing of cII mutants

We determined mutations in the lambda *cII* transgene using the DNA cycle sequencing method described elsewhere [15]. The *cII* gene region (294 bp) was PCR-amplified directly from mutant plaques using the primer pair 5′-AAAAAGGGCATCAAATTAAACC-3′ and 5′-CCGAAGTTGAGTATTTTTGCTGT-3′. A 446 bp PCR product was purified and used for the sequencing reaction with a BigDye™ Terminator Cycle Sequencing Kit (Applied Biosystems, Tokyo). PCR amplification and DNA sequencing was performed using a Program Temp Control System PC-800 (Astec, Tokyo) and an ABI Prism™ 310 Genetic Analyzer (Applied Biosystems), respectively.

2.7. Statistical analysis

We expressed MF as mean ± S.D. We compared between-group means by the unpaired *t*-test and variance among groups by one-way analysis of variance (ANOVA). We used the Dunnet test for multiple comparisons. Identical mutations from the same mouse were counted as a single event.

3. Results

3.1. Mutagenicity of PhIP

Comparison of *lacZ* MFs in the whole colon and colon epithelium of the same animals exposed to PhIP or corn oil (control) is shown in Fig. 1. The spontaneous MF in the colon epithelium was about twice that in the whole colon. The MF in the PhIP treatment group was significantly higher than in the control group in both the whole colon ($P < 0.05$) and the

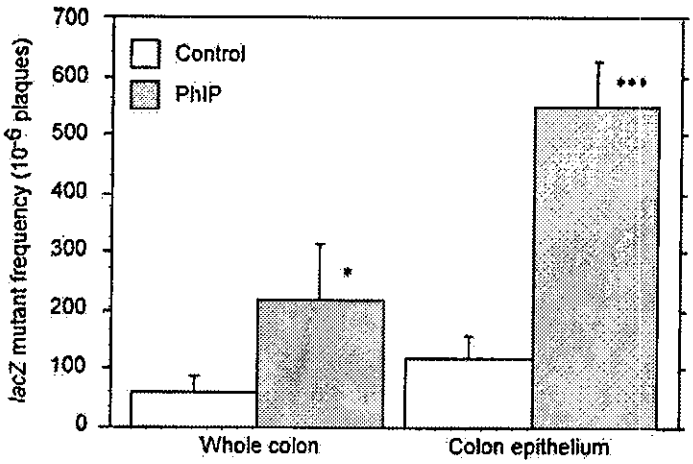

Fig. 1. *lacZ* mutant frequencies induced by PhIP in the whole colon and colon epithelium of male Muta™Mouse. The animals were orally fed 20 mg/kg PhIP or corn oil (control) daily for 5 days and sacrificed 2 weeks after the last administration. The MFs in the whole colon and colon epithelium of the same animals ($n = 5$) were analyzed. Asterisks indicate significantly different levels of induced MF in the control and PhIP treatment groups as determined by the unpaired *t*-test ($^{*}P < 0.05$, $^{***}P < 0.0005$). Values are mean ± S.D.

colon epithelium ($P < 0.0005$). Because the degree of increase in mean MF in treated animals was greater in the colon epithelium than in the whole colon (4.7 versus 3.5 times the control value, respectively), we used epithelium for the remainder of the experiments. The MFs in the PhIP treatment group were significantly higher than those in the control group in the epithelium of the small intestine, cecum, and colon (Fig. 2). The induced MFs did not differ significantly among the various sections of the organ (one-way ANOVA).

The effect of PhIP treatment on the MF of the *lacZ* and *cII* genes in the small intestine are shown in Table 1. The MF was lower for the *cII* gene than the *lacZ* gene in both control and PhIP-treated mice. The

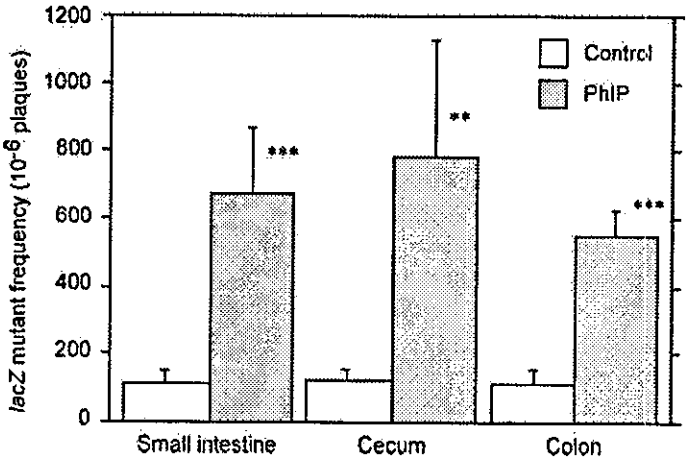

Fig. 2. *lacZ* mutant frequencies induced by PhIP in the intestinal epithelia of the small intestine, cecum, and colon. The animals are treated as described in the legend to Fig. 1. The MFs in the small intestines and ceca of seven animals were determined. Asterisks indicate significantly different levels of MF in the control and PhIP treatment groups as determined by the unpaired *t*-test ($^{**}P < 0.005$, $^{***}P < 0.0005$). Values are mean ± S.D.

Table 1
Spontaneous and PhIP-induced mutant frequencies of *lacZ* and *cII* loci in small intestine epithelium

Locus	Compound[a]	n[b]	Number of plaques		Mutant frequency[c]
			Total	Mutant	Mean ± S.D.
lacZ	Control	7	1909100	190	112.3 ± 30.6
	PhIP	7	1006992	741	672.0 ± 198.0[d]
cII	Control	6	1602500	54	49.6 ± 41.7
	PhIP	5	736000	165	199.4 ± 87.8[e]

[a] Animals were treated orally with 20 mg/kg per day PhIP for 5 days and killed 2 weeks after the last treatment.
[b] Number of analyzed animals.
[c] Mutant frequencies ($\times 10^{-6}$ plaques) were analyzed in DNA extracted from the small intestine epithelium.
[d] Significantly different from the control value at $P < 0.0005$.
[e] Significantly different from the control value at $P < 0.005$.

PhIP-induced increase in MF was six times the control value in the *lacZ* gene and four times the control value in the *cII* gene.

3.2. cII mutant sequences

We subjected 33 PhIP-induced mutants and 31 spontaneous mutants to sequence analysis. The mutations are characterized in Table 2 and summarized in Table 3. Spontaneous mutations from the control mice consisted mainly of base substitutions. G:C → A:T transitions were predominant, with 72% (13/18) occurring at 5′-CpG-3′ dinucleotide sequences. Other base substitutions (21%) and single base pair deletions (16%) were also observed. PhIP-induced mutations also consisted mainly of base substitutions (32/33), but the majority of those (72%) were G:C → T:A transversions compared with 8% of the spontaneous base substitutions. No obvious hot spots were seen, and mutations were distributed over the whole coding region.

3.3. Mutagenicity of IQ, MeIQ, and Trp-P-2

One-way ANOVA revealed a significant variance in the cecum and colon but not in the small intestine (Fig. 3). In the cecum (B), significant differences from the control were found in the IQ ($P < 0.0005$) and MeIQ groups (Dunnet test, $P < 0.0005$). The MFs in the IQ, MeIQ, and Trp-P-2 groups were 1.9, 2.7 and 1.4 times those of the control, respectively. MeIQ also significantly increased the MF in the colon (C) ($P < 0.0005$, Dunnet test). The MFs in the IQ and MeIQ groups were 1.5 and 3.1 times those of the control, respectively. We observed no significant increase in MF in any sample from the Trp-P-2 treatment group. We observed no significant variance in spontaneous MFs of the control groups in the colon, cecum, or small intestine (one-way ANOVA).

4. Discussion

In the transgenic mouse assays, isolation of proliferative tissues is important for sensitive detection of gene mutation, since DNA lesion (adduct formation, etc.) is fixed as a mutation during DNA repair and replication. In the present study, the isolated colon epithelium was more sensitive to PhIP than the whole colon (Fig. 1). The cell turnover in the epithelium is more proliferative than that in the other smooth muscle and connective tissues. The presence of resting or quiescent cells in the crude intestine could level down the apparent MFs, because the mutational target genes are rescued from not only proliferating cells, but also quiescent cells, which are in the inactive state of mutation fixation that arises as a consequence of DNA damage [16].

Almost uniform induction of *lacZ* mutation in the mouse intestine was reproduced in our experiments using the epithelia of the small intestine, cecum, and colon (Fig. 2). It is known that a long-term feeding of HCA in the diet is more effective for inducing mutations [5,9], but, as confirmed in this study, short-term exposure followed by appropriate

Table 2
PhIP-induced and spontaneous *cII* mutations from the small intestine epithelium of Muta™Mouse

Mutant no.	Position	Nucleotide change	CpG[a]	Sequence	Amino acid change
PhIP-induced mutants					
P1	3	G to T		ATG GTT CGT GCA AAC	Met to Ile
P2	25	G to T		CGC AAC GAG GCT CTA	Glu to Stop
P3	28	G to T		AAC GAG GCT CTA CGA	Ala to Ser
P4	34	C to T	*	GCT CTA CGA ATC GAG	Arg to Stop
P5	34	C to G		GCT CTA CGA ATC GAG	Arg to Gly
P6	35	G to C		GCT CTA CGA ATC GAG	Arg to Pro
P7	40	G to T		CGA ATC GAG AGT GCG	Glu to Stop
P8	40	G to A	*	CGA ATC GAG AGT GCG	Glu to Lys
P9	64	G to C		AAA ATC GCA ATG CTT	Ala to Pro
P10	88	G to T		AAG ACA GCG GAA GCT	Ala to Ser
P11	100	G to T		GCT GTG GGC GTT GAT	Gly to Cys
P12	103	ΔG		GTG GGC GTT GAT AAG	Frameshift
P13	111	G to T		GTT GAT AAG TCG CAG	Lys to Asn
P14	115	C to G		AAG TCG CAG ATC AGC	Gln to Glu
P15	115	C to T		AAG TCG CAG ATC AGC	Gln to Stop
P16	123	C to A		CAG ATC AGC AGG TGG	Ser to Arg
P17	125	G to T		ATC AGC AGG TGG AAG	Arg to Met
P18	134	G to T		TGG AAG AGG GAC TGG	Arg to Met
P19	145	C to A		TGG ATT CCA AAG TTC	Pro to Thr
P20	146	C to A		TGG ATT CCA AAG TTC	Pro to Gln
P21[b]	163	C to T		ATG CTG CTT GCT GTT	Lue to Phe
P22	163	C to A		ATC CTG CTT GCT GTT	Lue to Ile
P23	166	G to T		CTG CTT GCT GTT CTT	Ala to Ser
P24	167	C to A		CTG CTT GCT GTT CTT	Ala to Asp
P25	175	G to T		GTT CTT GAA TGG GGG	Glu to Stop
P26	179	G to T		CTT GAA TGG GGG GTC	Trp to Lue
P27	179	G to T		CTT GAA TGG GGG GTC	Trp to Lue
P28	193	G to A	*	GTT GAC GAC GAC ATG	Asp to Asn
P29	196	G to T		GAC GAC GAC ATG GCT	Asp to Thr
P30	210	G to T		GCT CGA TTG GCG CGA	Leu to Phe
P31	212	C to A		CGA TTG GCG CGA CAA	Ala to Glu
P32	220	G to T		CGA CAA GTT GCT GCG	Val to Phe
P33	220	G to T		CGA CAA GTT GCT GCG	Val to Phe
Spontaneous mutants					
C1	25	G to A	*	GCC AAC GAG GCT CTA	Glu to Lys
C2	34	C to T	*	GCT CTA CGA ATC GAG	Arg to Stop
C3	34	C to T	*	GCT CTA CGA ATC GAG	Arg to Stop
C4	40	G to A	*	CGA ATC GAG AGT GCG	Glu to Lys
C5	89	C to T	*	AAG ACA GCG GAA GCT	Ala to Val
C6	89	C to T	*	AAG ACA GCG GAA GCT	Ala to Val
C7	89	C to T	*	AAG ACA GCG GAA GCT	Ala to Val
C8	94	G to T		GCG GAA GCT GTG GGC	Ala to Ser
C9	94	G to A		GCG GAA GCT GTG GGC	Ala to Thr
C10	101	G to A		GCT GTG GGC GTT GAT	Gly to Asp
C11	101	G to C		GCT GTG GGC GTT GAT	Gly to Ala
C12	113	C to T	*	GAT AAG TCG CAG ATC	Ser to Leu
C13	113	C to T	*	GAT AAG TCG CAG ATC	Ser to Leu
C14	116	A to G		AAG TCG CAG ATC AGC	Gln to Arg
C15	123	C to A		CAG ATC AGC AGG TGG	Ser to Arg
C16	125	G to A		ATC AGC AGG TGG AAG	Arg to Lys
C17	131	A to C		AGG TGG AAG AGG GAC	Lys to Thr

Table 2 (*Continued*)

Mutant no.	Position	Nucleotide change	CpG[a]	Sequence	Amino acid change
C18	150	ΔG		ATT CCA AAG TTC TCA	Frameshift
C19	163	ΔC		ATC CTG CTT GCT GTT	Frameshift
C20	170	T to G		CTT GCT GTT CTT GAA	Val to Gly
C21	179–184	ΔG		GAA TGG GGG GTC GTT	Frameshift
C22	183–184	GG to T		GAA TGG GGG TC GTT	Frameshift
C23	196	G to A	*	GAC GAC GAC ATG GCT	Asp to Asn
C24	214	C to T	*	TTG GCG CGA CAA GTT	Arg to Stop
C25	214	C to T	*	TTG GCG CGA CAA GTT	Arg to Stop
C26	214	C to T	*	TTG GCG CGA CAA GTT	Arg to Stop
C27	217	C to T		GCG CGA CAA GTT GCT	Gln to Stop
C28	217	C to T		GCG CGA CAA GTT GCT	Gln to Stop
C29	220	G to C		CGA CAA GTT GCT GCG	Val to Leu
C30	241–246	ΔA		ACC AAT AAA AAA AAA CGC	Frameshift
C31	249–251	ΔC		AAA CGC CCG GCG GCA	Frameshift

[a] C to T transition at CpG site (*).
[b] Identical mutation from same mouse.

expression (manifestation) time is sufficient to induce gene mutation in the intestinal epithelia.

In the *cII* gene in the small intestinal epithelium of the male Muta^{TM}Mouse, PhIP was the only HCA that increased MF (Table 1 and Fig. 3). MeIQ induced *cII* mutations in the cecum and colon, but IQ was mutagenic only in the cecum. In both the cecum and colon, the MFs induced by MeIQ were higher than those induced by IQ. PhIP, in contrast, induced MFs uniformly throughout the intestinal tract. These results suggest that PhIP is the most potent mutagen for the mouse intestine, followed by MeIQ and then IQ (Trp-P-2 was not mutagenic), and the epithelium in the cecum is the most susceptible to HCAs.

Table 3
Classification of PhIP-induced and spontaneous *cII* mutations from small intestine epithelium of Muta^{TM}Mouse

Mutation type	PhIP-induced		Spontaneous	
	Number	%	Number	%
Base substitutions				
Transitions				
G:C to A:T (at CpG)	5 (3)	15 (9)	18 (13)	58 (42)
A:T to G:C	0	0	1	3
Transversions				
A:T to T:A	0	0	0	0
A:T to C:G	0	0	2	6
G:C to T:A	23	70	2	6
G:C to C:G	4	12	2	6
Single base pair deletion				
G:C	1	3	5	16
A:T	0	0	0	0
Other mutations	0	0	1	3
Total[a]	33	100	31	100

[a] Identical mutations from the same mouse were counted as single event.

The reasons for regional differences in HCA susceptibility are not clear. Differences of the distribution of DNA adducts may play a role. Metabolic activation leading to the formation of DNA adducts is critical to the genotoxicity of HCAs. These compounds are first metabolized by cytochrome P450 and are converted in the liver to *N*-hydroxy intermediates and released back into the gut [17]. The intermediates are converted into ultimate mutagens, capable of binding to DNA in the intestinal epithelium. The distribution of ^{32}P-post-labeled DNA adducts in the small intestine, cecum, and colon of male CDF1 mice given dietary PhIP are almost the same [18]. The distribution in those given IQ, on the other hand, is higher in the cecum than in the colon, and IQ-DNA adduct formation is lowest in the small intestine [19]. Such differences in the distribution of DNA adducts may help to explain the tissue-specific difference in HCA-induced mutagenesis.

The regional differences in HCA susceptibility were shown in the intestine of the male CDF1 Muta^{TM}Mouse, but mutation alone is not sufficient to explain differences in carcinogenicity. PhIP induces

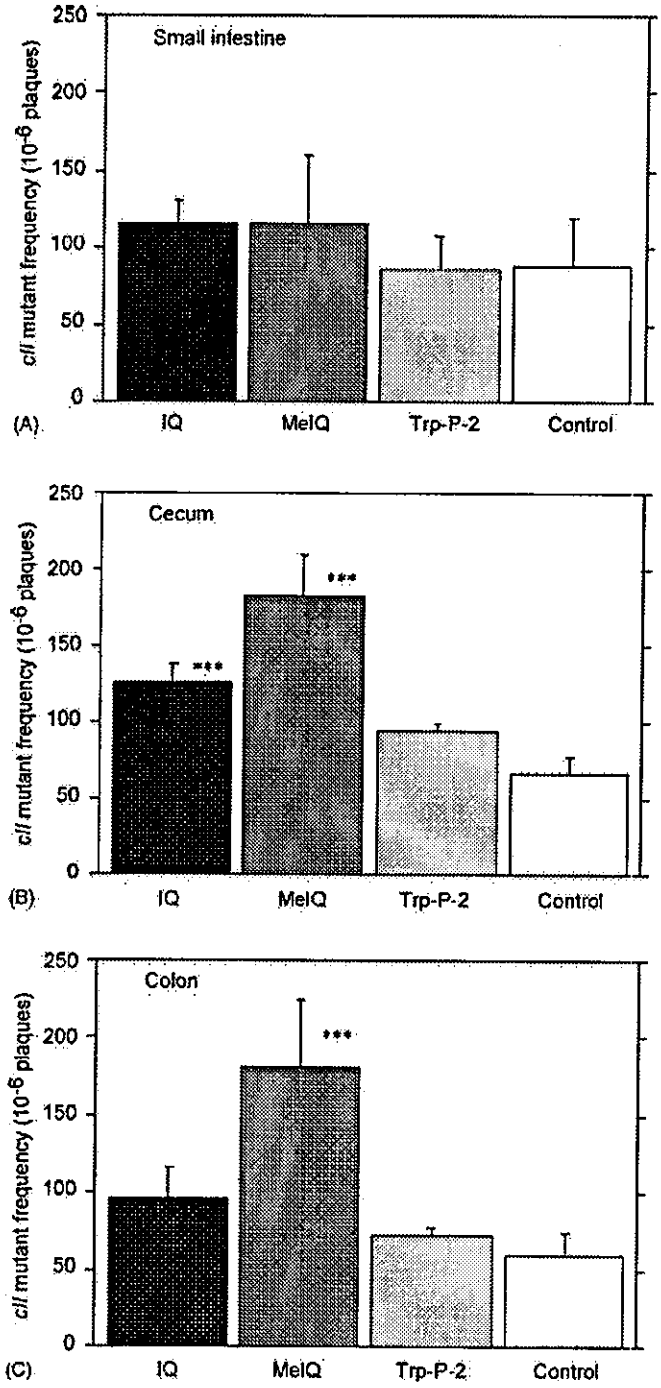

Fig. 3. *cII* mutant frequencies induced by IQ, MeIQ, and Trp-P-2 in the epithelium of small intestine (A), cecum (B) and colon (C). The animals were fed 20 mg/kg HCA or corn oil (control) daily for 5 days and sacrificed 2 weeks after the last dose. The MFs in the same animals ($n = 4$–5) in each treatment group were analyzed. Asterisks indicate significantly different levels of MF in the control and HCA treatment groups as determined by Dunnet's test ($P < 0.0005$). Values are mean ± S.D.

colon cancer in male F344 rats but not in females [20] and not in either sex of CDF1 [21] and C57BL/6 mice [22], yet there is no marked difference in the frequency and spectrum of *lacI* mutations in the colon of both sexes of C57BL/6 Big Blue® mice and F344 Big Blue® rats [23]. In the present study (Tables 2 and 3), analysis of the *cII* mutants recovered from the small intestine of PhIP-treated Muta™Mice showed that the mutations were similar to those induced by PhIP in the colons of Big Blue® rats, where G:C → T:A and G:C → C:G transversions were induced in both the *cII* [24] and *lacI* genes [25]. Thus, these mutational characteristics have been well conserved between the small intestine of mice and the large intestine of rats, although the organs differ in susceptibility to PhIP carcinogenicity.

MeIQ is an intestinal carcinogen in female C57BL/6 mice but not in male or female CDF1 mice [26,27], and it induces *lacI* mutations in the colon of female Big Blue® mice [8]. Although we used the male CDF1 Muta™Mouse in the present study, MeIQ significantly induced *cII* mutations in the cecum and colon. IQ induces tumors in the large and small intestines of F344 rats but not of CDF1 mice [28], and it induces *lacI* mutations in the colon of Big Blue® rats [29]. We believe that the present study is the first to show IQ mutagenicity in the mouse intestine. The difference in the intestinal carcinogenicity of HCAs was not attributable to differences in mutational specificity in the intestinal epithelia but might be due to differences in a post-initiation stage in carcinogenesis.

Since two non-transcribed transgenes such as *lacZ* and lambda *cII* are not expected to differ in rates of DNA damage or repair, it is tempting to attribute the differences in mutagenic responses observed in this study to differences in either target size or sequence context. The spontaneous MF of the *cII* gene was about a half that of *lacZ* gene even though the *cII* was much smaller than *lacZ* (294 bp versus 3096 bp), suggesting that *cII* is more mutable than *lacZ*. In response to PhIP treatment, however, *cII* and *lacZ* were nearly identical. Observations made with other mutagenic chemicals also suggest that the response of the *cII* gene is similar to that of the *lacZ* gene [30–32].

In both *lacI* of Big Blue® mice and *lacZ* of Muta™Mice, PhIP preferentially induces single G:C base pair deletions in the sequence 5′-GGGA-3′ [24,25,33]. The *cII* gene, however, contains only one 5′-GGGA-3′ sequence, and we found no PhIP mutational hot spot. Although all 33 PhIP-induced mutants in this study had a G:C base pair mutation, we found no increase in the frequency of PhIP-induced G:C base pair deletions. This has been also demonstrated in the *cII* and *lacI* genes in the Big Blue® rat colon [24]. Compared with the spontaneous mutational spectra from the colons of untreated rats, the proportion of −1 frameshifts (almost exclusively deletion of a G:C base pair) in PhIP-induced mutants is elevated more than 10-fold in the *lacI* but not the *cII* gene [24]. This suggests that *cII* differs from *lacZ* and *lacI* in its mutagenic response to PhIP.

Acknowledgements

This study was supported in part by a Grant-in-Aid for Environmental Pollution Research from the Ministry of the Environment, Japan.

References

[1] L.S. Gold, T.H. Slone, B.R. Stern, L. Bernstein, Comparison of target organs of carcinogenicity for mutagenic and non-mutagenic chemicals, Mutat. Res. 286 (1993) 75–100.
[2] M. Nagao, T. Sugimura, Carcinogenic factors in food with relevance to colon cancer development, Mutat. Res. 290 (1993) 43–51.
[3] L.S. Gold, T.H. Slone, N.B. Manley, B.N. Ames, Heterocyclic amines formed by cooking food: comparison of bioassay results with other chemicals in the carcinogenic potency database, Cancer Lett. 83 (1994) 21–29.
[4] R.A. Brooks, N.J. Gooderham, K. Zhao, R.J. Edwards, L.A. Howard, A.R. Boobis, D.J. Winton, 2-Amino-1-methyl-6-phenylimidazo[4,5-*b*]pyridine is a potent mutagen in the mouse small intestine, Cancer Res. 54 (1994) 1665–1671.
[5] X.B. Zhang, J.S. Felton, J.D. Tucker, C. Urlando, J.A. Heddle, Intestinal mutagenicity of two carcinogenic food mutagens in transgenic mice: 2-amino-1-methyl-6-phenylimidazo[4,5-*b*]pyridine and amino(α)carboline, Carcinogenesis 17 (1996) 2259–2265.
[6] A.M. Lynch, N.J. Gooderham, A.R. Boobis, Organ distinctive mutagenicity in Muta™Mouse after short-term exposure to PhIP, Mutagenesis 11 (1996) 505–509.
[7] K. Masumura, K. Matsui, M. Yamada, M. Horiguchi, K. Ishida, M. Watanabe, O. Ueda, H. Suzuki, Y. Kanke, K.R. Tindall, K. Wakabayashi, T. Sofuni, T. Nohmi, Mutagenicity of 2-amino-1-methyl-6-phenylimidazo[4,5-*b*]pyridine (PhIP) in the new *gpt Δ* transgenic mouse, Cancer Lett. 143 (1999) 241–244.

[8] T. Suzuki, M. Hayashi, M. Ochiai, K. Wakabayashi, T. Ushijima, T. Sugimura, M. Nagao, T. Sofuni, Organ variation in the mutagenicity of MeIQ in Big Blue® *lacI* transgenic mice, Mutat. Res. 369 (1996) 45–49.
[9] T. Itoh, T. Suzuki, A. Nishikawa, F. Furukawa, M. Takahashi, W. Xue, T. Sofuni, M. Hayashi, In vivo genotoxicity of 2-amino-3,8-dimethylimidazo[4, 5-*f*]quinoxaline in *lacI* transgenic (Big Blue®) mice, Mutat. Res. 468 (2000) 19–25.
[10] J.A. Gossen, W.J.F. De Leeuw, C.H.T. Tan, E.C. Zwarthoff, F. Berends, P.H.M. Lohman, D.L. Knook, J. Vijg, Efficient rescue of integrated shuttle vectors from transgenic mice: a model for studying mutations in vivo, Proc. Natl. Acad. Sci. U.S.A. 86 (1989) 7971–7975.
[11] L.S. Gold, C.B. Sawyer, R. Magaw, G.M. Backman, M. de Veciana, R. Levinson, N.K. Hooper, W.R. Havender, L. Bernstein, R. Peto, M.C. Pike, B.N. Ames, A carcinogenic potency database of the standardized results of animal bioassays, Environ. Health Perspect. 58 (1984) 9–319.
[12] T. Suzuki, T. Itoh, M. Hayashi, Y. Nishikawa, S. Ikezaki, F. Furukawa, M. Takahashi, T. Sofuni, Organ variation in the mutagenicity of dimethylnitrosamine in Big Blue® mice, Environ. Mol. Mutagen. 28 (1996) 348–353.
[13] The Collaborative Study Group for the Transgenic Mouse Mutation Assay, Mammalian Mutagenesis Study Group of the Environmental Mutagen Society of Japan, Organ variation in the mutagenicity of ethylnitrosourea in Muta™Mouse: results of the collaborative study on the transgenic mutation assay by JEMS/MMS. Environ. Mol. Mutagen. 28 (1996) 363–375.
[14] J.L. Jakubczak, G. Merlino, J.E. French, W.J. Muller, B. Paul, S. Adhya, S. Garges, Analysis of genetic instability during mammary tumor progression using a novel selection-based assay for in vivo mutations in a bacteriophage λ transgene target, Proc. Natl. Acad. Sci. U.S.A. 93 (1996) 9073–9078.
[15] T. Suzuki, X. Wang, Y. Miyata, K. Saeki, A. Kohara, Y. Kawazoe, M. Hayashi, T. Sofuni, Hepatocarcinogen quinoline induces G:C to C:G transversions in the *cII* gene in the liver of lambda/*lacZ* transgenic mice (Muta™Mouse), Mutat. Res. 456 (2000) 73–81.
[16] J.H. Bielas, J.A. Heddle, Proliferation is necessary for both repair and mutation in transgenic mouse cells, Proc. Natl. Acad. Sci. U.S.A. 97 (2000) 11391–11396.
[17] R. Kato, Metabolic activation of mutagenic heterocyclic aromatic amines from protein pyrolysates, CRC Crit. Rev. Toxicol. 16 (1986) 307–348.
[18] S. Josyula, H.A. Schut, Dietary omega-3 fatty acids as potential inhibitors of carcinogenesis: effect on DNA adduct formation of 2-amino-1-methyl-6-phenylimidazo[4,5-*b*]pyridine (PhIP) in mice and rats, Food Chem. Toxicol. 37 (1999) 287–296.
[19] H.A. Schut, C.L. Wang, L.M. Twining, K.M. Earle, Formation and persistence of DNA adducts of 2-amino-3-methylimidazo [4,5-*f*]quinoline (IQ) in CDF1 mice fed a high ω-3 fatty acid diet, Mutat. Res. 378 (1997) 23–30.
[20] N. Ito, R. Hasegawa, M. Sano, S. Tamano, H. Esumi, S. Takayama, T. Sugimura, A new colon and mammary carcinogen in cooked food, 2-amino-1-methyl-6-phenylimidazo[4,5-*b*]pyridine (PhIP), Carcinogenesis 12 (1991) 1503–1506.
[21] H. Esumi, H. Ohgaki, E. Kohzen, S. Takayama, T. Sugimura, Induction of lymphoma in CDF1 mice by the food mutagen, 2-amino-1-methyl-6-phenylimidazo[4,5-*b*]pyridine, Jpn. J. Cancer Res. 80 (1989) 1176–1178.
[22] E. Kristiansen, A. Mortensen, I.K. Sørensen, Effects of long-term feeding with 2-amino-1-methyl-6-phenylimidazo[4,5-*b*]pyridine (PhIP) in C57BL/ByA and Eμ-*pim*-1 mice, Cancer Lett. 122 (1998) 215–220.
[23] H. Okonogi, G.R. Stuart, E. Okochi, T. Ushijima, T. Sugimura, B.W. Glickman, M. Nagao, Effects of gender and species on spectra of mutation induced by 2-amino-1-methyl-6-phenylimidazo[4,5-*b*]pyridine in the *lacI* transgene, Mutat. Res. 395 (1997) 93–99.
[24] G.R. Stuart, E. Thorleifson, E. Okochi, J.G. de Boer, T. Ushijima, M. Nagao, B.W. Glickman, Interpretation of mutational spectra from different genes: analyses of PhIP-induced mutational specificity in the *lacI* and *cII* transgenes from colon of Big Blue® rats, Mutat. Res. 452 (2000) 101–121.
[25] G.R. Stuart, J.G. de Boer, R. Haesevoets, J. Holcroft, J. Kangas, K. Sojonky, E. Thorleifson, A. Thornton, D.F. Walsh, H. Yang, B.W. Glickman, Mutations induced by 2-amino-1-methyl-6-phenylimidazo[4,5-*b*]pyridine (PhIP) in cecum and proximal and distal colon of *lacI* transgenic rats, Mutagenesis 16 (2001) 431–437.
[26] H. Fujita, K. Nagano, M. Ochiai, T. Ushijima, T. Sugimura, M. Nagao, T. Matsushima, Difference in target organs in carcinogenesis with a heterocyclic amine, 2-amino-3,4-dimethylimidazo[4,5-*f*]quinoline, in different strains of mice, Jpn. J. Cancer Res. 90 (1999) 1203–1206.
[27] H. Ohgaki, H. Hasegawa, M. Suenaga, T. Kato, S. Sato, S. Takayama, T. Sugimura, Induction of hepatocellular carcinoma and highly metastatic squamous cell carcinomas in the forestomach of mice by feeding 2-amino-3,4-dimethylimidazo[4,5-*f*]quinoline, Carcinogenesis 7 (1986) 1889–1893.
[28] H. Ohgaki, H. Hasegawa, T. Kato, M. Suenaga, M. Ubukata, S. Sato, S. Takayama, T. Sugimura, Carcinogenicity in mice and rats of heterocyclic amines in cooked foods, Environ. Health Perspect. 67 (1986) 129–134.
[29] S.A.M. Bol, J. Horlbeck, J. Markovic, J.G. de Boer, R.J. Turesky, A. Constable, Mutational analysis of the liver, colon and kidney of Big Blue® rats treated with 2-amino-3-methylimidazo[4,5-*f*]quinoline, Carcinogenesis 21 (2000) 1–6.
[30] A. Kohara, T. Suzuki, M. Honma, N. Hirano, K. Ohsawa, T. Ohwada, M. Hayashi, Mutation spectrum of *o*-aminoazotoluene in the *cII* gene of lambda/*lacZ* transgenic mice (Muta™Mouse), Mutat. Res. 491 (2001) 211–220.
[31] A. Kohara, T. Suzuki, M. Honma, T. Oomori, T. Ohwada, M. Hayashi, Dinitropyrenes induce gene mutations in multiple organs of the lambda/*lacZ* transgenic mouse (Muta™Mouse), Mutat. Res. 515 (2002) 73–83.
[32] A. Kohara, T. Suzuki, M. Honma, T. Ohwada, M. Hayashi, Mutagenicity of aristolochic acid in the lambda/*lacZ* transgenic mouse (Muta™Mouse), Mutat. Res. 515 (2002) 63–72.
[33] A.M. Lynch, N.J. Gooderham, D.S. Davies, A.R. Boobis, Genetic analysis of PhIP intestinal mutations in Muta™-Mouse, Mutagenesis 13 (1998) 601–605.

Available online at www.sciencedirect.com
SCIENCE DIRECT®
Mutation Research 559 (2004) 83–95
Genetic Toxicology and Environmental Mutagenesis
www.elsevier.com/locate/gentox
Community address: www.elsevier.com/locate/mutres

In vivo mutagenicity of benzo[*f*]quinoline, benzo[*h*]quinoline, and 1,7-phenanthroline using the *lacZ* transgenic mice

Katsuya Yamada[a], Takayoshi Suzuki[b], Arihiro Kohara[a,b], Makoto Hayashi[b], Takaharu Mizutani[a], Ken-Ichi Saeki[a,*]

[a] *Graduate School of Pharmaceutical Sciences, Nagoya City University, Tanabedori, Mizuho-ku, Nagoya 467-8603, Japan*
[b] *Division of Genetics and Mutagenesis, National Institute of Health Sciences, 1-18-1 Kamiyoga, Setagaya-ku, Tokyo 158-8501, Japan*

Received 25 September 2003; received in revised form 26 December 2003; accepted 26 December 2003

Abstract

Phenanthrene, a simplest angular polycyclic aromatic hydrocarbon with a bay-region in its molecule, is reported to be non-mutagenic, although most angular (non-linear) polycyclic aromatic hydrocarbons, such as benzo[*a*]pyrene and chrysene, are known to show genotoxicity after metabolic transformation into a bay-region diol epoxide. On the other hand, benzo[*f*]quinoline (BfQ), benzo[*h*]quinoline (BhQ), and 1,7-phenanthroline (1,7-Phe), which are all aza-analogs of phenanthrene, are mutagenic in the Ames test using *Salmonella typhimurium* TA100 in the presence of a rat liver S9 fraction. In this report, we undertook to investigate the in vivo mutagenicity of BfQ, BhQ and 1,7-Phe by an in vivo mutation assay system using the *lacZ* transgenic mouse (Muta™Mouse). BfQ and BhQ only slightly induced mutation in the liver and lung, respectively. BfQ- and BhQ-induced *cII* mutant spectra showed no characteristics compared with that of the control. These results suggest that the in vivo mutagenicities of BfQ and BhQ were equivocal. On the other hand, 1,7-Phe induced a potent mutation in the liver and a weak mutation in the lung. Furthermore 1,7-Phe depressed the G:C to A:T transition and increased the G:C to C:G transversion in the liver like quinoline, a hepatomutagen possessing the partial structure of 1,7-Phe, compared with the spontaneous mutation spectrum. These results suggest that the in vivo mutagenicity of 1,7-Phe might be caused by the same mechanism as that of quinoline, which induced the same mutational spectrum change (G:C to C:G transversion).

Keywords: Tricyclic aza-arene; In vivo mutagenesis assay; Mutation spectrum

1. Introduction

Carcinogenic aza-arenes are widely distributed in the environmental pollutants such as cigarette smoke [1] and urban air [2–4]. Although numerous studies about the in vitro mutagenicity of aza-arenes have been reported, the metabolic activation mechanism of aza-arenes has not yet been elucidated, except for that of heterocyclic amines. Furthermore, there are only a few reports about the in vivo mutagenicity of aza-arenes. We have investigated the in vitro and in vivo mutagenicity of aza-arenes with special attention to their metabolic activation mechanisms. 10-Azabenzo[*a*]pyrene, a carcinogenic aza-analog [5] of benzo[*a*]pyrene, was reported to be as mutagenic as benzo[*a*]pyrene in the Ames test using *Salmonella typhimurium* TA100 in the presence of a rat liver S9 fraction [6–8]. In our previous study,

* Corresponding author. Tel.: +81-52-836-3485; fax: +81-52-834-9309.
E-mail address: saeki@phar.nagoya-cu.ac.jp (K.-I. Saeki).

1383-5718/$ – see front matter © 2004 Elsevier B.V. All rights reserved.
doi:10.1016/j.mrgentox.2003.12.012

Fig. 1. Structures of BfQ, BhQ and 1,7-Phe.

10-azabenzo[*a*]pyrene showed significant mutagenicity only in the liver and colon in an in vivo mutation assay system using the *lacZ* transgenic mouse (Muta^{TM}Mouse) [9]. We have also reported that the total dose of 200 mg/kg (50 mg/kg per day × 4 days) of quinoline, a hepatocarcinogenic [10,11] aza-analog of naphthalene, showed a potent mutagenicity and induced primarily G:C to C:G transversions in the liver of Muta^{TM}Mouse [12–14].

Phenanthrene, a simplest angular polycyclic aromatic hydrocarbon with a bay-region in its molecule, has been reported to be non-mutagenic [15], although most angular (non-linear) polycyclic aromatic hydrocarbons, such as benzo[*a*]pyrene and chrysene, are known to show genotoxicity after metabolic transformation into a bay-region diol epoxide. On the other hand, it was reported that benzo[*f*]quinoline (BfQ) and 1,7-phenanthroline (1,7-Phe) (Fig. 1), which are environmental contaminants and aza-analogs of phenanthrene, were mutagenic in the Ames test using *S. typhimurium* TA100 in the presence of a rat liver S9 fraction [16–18]. Furthermore, benzo[*h*]quinoline (BhQ) (Fig. 1), a positional isomer of BfQ, was reported to be weakly or equivocally mutagenic in *S. typhimurium* TA100 with a rat liver S9 fraction [19,20]. In our previous report, it was suggested that metabolic activation of these tricyclic aza-arenes might take place in the pyridine moiety, like quinoline, to form the ultimate genotoxic form, an enamine epoxide (*N*,d-hydrated a,b-epoxide) (Fig. 2) [18].

In the present study, we undertook to investigate the in vivo mutagenicity of BfQ, BhQ and 1,7-Phe by the in vivo mutation assay system using the *lacZ* transgenic mouse (Muta^{TM}Mouse).

2. Materials and methods

2.1. Materials

BfQ (CAS Registry No. 85-02-9) and BhQ (CAS Registry No. 230-27-3) were purchased from Tokyo Kasei Kogyo Co. Ltd. (Tokyo), 1,7-Phe (CAS Registry No. 230-46-6) from Aldrich, phenyl-β-D-galactoside (P-gal) from Sigma Chemical Co. (St. Louis, MO, USA), proteinase K and olive oil from Wako Pure Chemicals (Osaka), and RNase from Boeringer Mannheim.

2.2. In vivo mutagenesis assay using Muta^{TM}Mouse

2.2.1. Animals and treatments

Seven-week-old male Muta^{TM}Mice, supplied by COVANCE Research Products (PA, USA), were acclimatized for 1 week before use and divided into seven groups of four mice each. BfQ, BhQ, and 1,7-Phe dissolved in olive oil (10 ml/kg body weight) were injected intraperitoneally into two, one, and two groups, respectively, at single doses of 100, 100, and 50 mg/kg, respectively, for four consecutive days. The remaining two groups were given olive oil as the control.

2.2.2. Tissues and DNA isolation

All mice were killed by cervical dislocation 14 days (BfQ-, BhQ-, 1,7-Phe- and olive oil-treated groups) or 56 days (BfQ-, 1,7-Phe- and olive oil-treated groups) after the last injection of a test chemical. The liver, spleen, lung, kidney, and bone marrow were immedi-

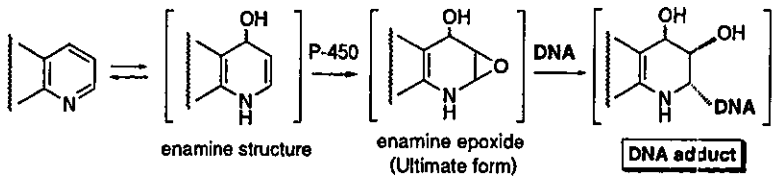

Fig. 2. Proposed metabolic activation pathway for the pyridine moiety (enamine epoxide theory).

ately extirpated, frozen in liquid nitrogen, and stored at −80 °C until DNA extraction. The genomic DNA was extracted from each tissue by the phenol/chloroform method as previously reported [12]. The isolated DNA was precipitated with ethanol, air-dried, and dissolved in an appropriate volume (20–200 μl) of TE-4 buffer (10 mM Tris–HCl at pH 8.0 containing 4 mM EDTA) at room temperature overnight. The DNA solution thus prepared was stored at 4 °C.

2.2.3. In vitro packaging

The lambda gt10/*lacZ* vector was efficiently recovered by the in vitro packaging reactions [21]. Our home-made (HM) packaging extract consisting of a sonic extract (SE) of *Escherichia coli* NM759 and a freeze–thaw lysate (FTL) of *E. coli* BHB2688 was prepared according to the methods of Gunther et al. [22]. As the general procedure for handling the HM extract, approximately 5 μg DNA was mixed with 15 μl of FTL and 30 μl of SE and incubated at 37 °C for 90 min. Then the SE and FTL were combined again and the mixture was incubated for another 90 min. The reaction was terminated by the addition of an appropriate volume of SM buffer (50 mM Tris–HCl at pH 7.5, 10 mM $MgSO_4$, 100 mM NaCl, 0.01% gelatin) and stored at 4 °C. By this procedure, the λgt10 vector was efficiently rescued from genomic DNA to form an infectious phage.

2.2.4. Mutation assays

2.2.4.1. lacZ mutant frequency determination. The positive selection for *lacZ* mutants was performed as previously reported [12,23]. Briefly, the phage solution was absorbed to *E. coli* C (*lac*$^-$ *galE*$^-$) at room temperature for 20–30 min. For titration, an aliquot of the phage-*E. coli* solution was mixed with LB top agar (containing 10 mM $MgSO_4$) and plated onto dishes containing bottom agar. The remaining phage-*E. coli* solution was mixed with LB top agar containing phenyl-β-D-galactoside (P-gal) (3 mg/ml) and plated as described above. The mutant frequency (MF) was calculated by the following formula:

$$\text{mutant frequency} = \left(\frac{\text{total number of plaques on selection plates}}{\text{total number of plaques on titer plates}}\right) \times \text{dilution factor.}$$

The significance of differences in the mutant frequency between the treated and control groups was analyzed by using Student's *t*-test.

2.2.4.2. cII mutant frequency determination. We also examined the mutagenicity in the lambda *cII* gene integrated as a lambda vector gene, which serves as another selective marker as reported previously in the *lacI* transgenic BigBlue mouse [24]. The positive

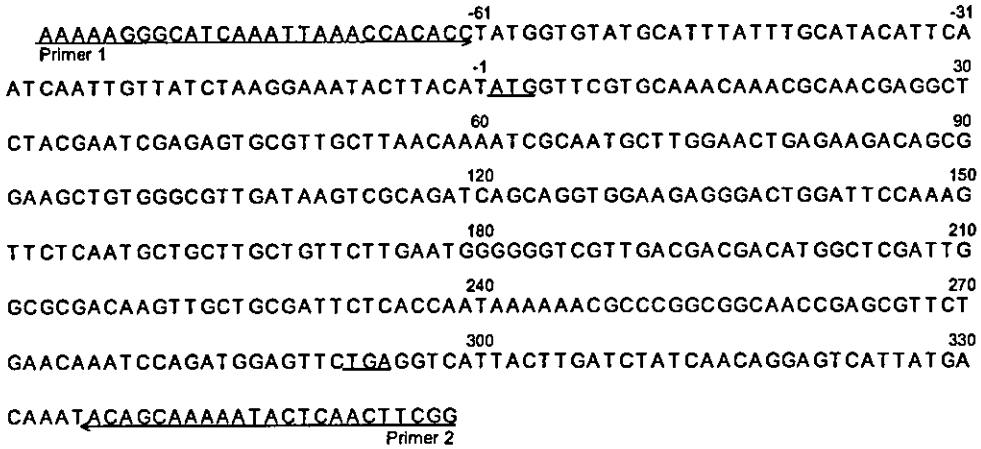

Fig. 3. Sequence map of the *cII* gene. The primers, used for PCR amplification and sequencing, are shown by arrows. The PCR gives 446 bp products that involve the entire (294 bp) *cII* gene. Initiation and stop codons are underlined.

Table 1
Mutant frequencies induced by BfQ, BhQ and 1,7-Phe in five organs of Muta™Mouse for the expression time of 14 days

Tissue	Treatment	*lacZ* assay				*cII* assay			
		Individual animal data			Average ± S.D.	Individual animal data			Average ± S.D.
		No. of phages analyzed	No. of mutants	MF × 10^5	MF × 10^5	No. of phages analyzed	No. of mutants	MF × 10^5	MF × 10^5
Liver	Control (olive oil)	1120000	106	9.5	7.0 ± 1.6	449400	12	2.7	2.1 ± 0.6
		816000	59	7.2		938400	24	2.6	
		1198000	73	6.1		764400	11	1.4	
		791500	41	5.2		699000	11	1.6	
	BfQ	634500	32	5.0	9.6 ± 3.1	804600	12	1.5	3.8 ± 1.6
		590000	51	8.6		662400	35	5.3	
		158500	20	12.6		426300	23	5.4	
		221500	27	12.2		883200	28	3.2	
	BhQ	442000	29	6.6	5.9 ± 1.1	1188000	53	4.5	2.6 ± 1.1
		677000	39	5.8		1134600	21	1.9	
		257500	11	4.3		671700	17	2.5	
		645500	46	7.1		1011000	15	1.5	
	1,7-Phe	272000	41	15.1	15.9 ± 0.5**	813600	44	5.4	4.1 ± 0.8*
		183000	30	16.4		562800	19	3.4	
		263000	43	16.3		720000	25	3.5	
		184000	29	15.8		606000	25	4.1	
Spleen	Control (olive oil)	855500	116	13.6	7.3 ± 3.6	623100	12	1.9	2.4 ± 0.3
		533000	29	5.4		1502400	41	2.7	
		446500	25	5.6		546900	15	2.7	
		461000	22	4.8		569400	13	2.3	
	BfQ	210500	13	6.2	6.1 ± 0.6	2098200	25	1.2	3.5 ± 2.8
		244500	16	6.5		441000	13	2.9	
		403000	27	6.7		785400	65	8.3	
		256500	13	5.1		786600	13	1.7	
	BhQ	297000	12	4.0	6.5 ± 1.6	277800	10	3.6	2.9 ± 0.6
		354500	25	7.1		828300	22	2.7	
		396500	26	6.6		946200	31	3.3	
		544000	46	8.5		1608600	34	2.1	
	1,7-Phe	426500	34	8.0	7.0 ± 1.0	967200	20	2.1	2.4 ± 0.7
		502500	27	5.4		1023000	24	2.3	
		320000	24	7.5		1026900	16	1.6	
		462500	34	7.4		905400	32	3.5	
Lung	Control (olive oil)	1539500	127	8.2	6.0 ± 1.3	1027800	21	2.0	2.1 ± 0.4
		1111500	60	5.4		738000	21	2.8	
		678000	35	5.2		1142700	20	1.8	
		1473000	76	5.2		831600	15	1.8	
	BfQ	553000	39	7.1	6.0 ± 0.6	1107600	18	1.6	2.6 ± 0.6
		332000	18	5.4		903300	22	2.4	
		353000	21	5.9		1124700	36	3.2	
		266000	15	5.6		445200	14	3.1	
	BhQ	401500	51	12.7	10.8 ± 2.4*	1705500	37	2.2	3.5 ± 1.0
		481500	54	11.2		1071000	33	3.1	
		572500	72	12.6		2403000	99	4.1	
		372000	25	6.7		2083200	98	4.7	

Table 1 (*Continued*)

Tissue	Treatment	*lacZ* assay				*cII* assay			
		Individual animal data			Average ± S.D.	Individual animal data			Average ± S.D.
		No. of phages analyzed	No. of mutants	MF × 10^5	MF × 10^5	No. of phages analyzed	No. of mutants	MF × 10^5	MF × 10^5
	1,7-Phe	335500	29	8.6	10.3 ± 1.9*	1103400	26	2.4	2.9 ± 0.5
		351000	46	13.1		1012200	27	2.7	
		244500	27	11.0		909600	34	3.7	
		211000	18	8.5		892200	26	2.9	
Kidney	Control (olive oil)	219500	15	6.8	6.8 ± 1.4	551100	21	3.8	2.7 ± 1.0
		190000	17	8.9		426600	16	3.8	
		349500	17	4.9		588000	11	1.9	
		301000	20	6.6		771000	12	1.6	
	BfQ	682500	46	6.7	7.4 ± 1.1	1035000	25	2.4	3.9 ± 0.9
		550500	51	9.3		825000	36	4.4	
		474000	33	7.0		649800	30	4.6	
		484000	32	6.6		1599000	66	4.1	
	BhQ	920500	55	6.0	7.4 ± 1.2	1323600	26	2.0	2.2 ± 0.5
		622000	51	8.2		945000	27	2.9	
		113000	10	8.8		1408800	23	1.6	
		244500	16	6.5		1018200	23	2.3	
	1,7-Phe	486500	30	6.2	6.8 ± 0.5	814800	15	1.8	3.3 ± 1.6
		558000	38	6.8		660300	40	6.1	
		177000	12	6.8		520200	13	2.5	
		319500	24	7.5		1664700	48	2.9	
Bone marrow	Control (olive oil)	311000	32	10.3	7.1 ± 3.0	644100	14	2.2	1.3 ± 0.6
		465000	27	5.8		1041000	16	1.5	
		70500	2	2.8		111300	1	0.9	
		96500	9	9.3		154500	1	0.6	
	BfQ	325500	17	5.2	6.4 ± 0.9	1075200	16	1.5	2.6 ± 0.9
		256500	17	6.6		528000	12	2.3	
		326000	25	7.7		572100	22	3.8	
		708500	44	6.2		1144800	32	2.8	
	BhQ	257000	13	5.1	5.7 ± 0.5	1757100	20	1.1	1.7 ± 0.4
		617000	38	6.2		1349400	24	1.8	
		683000	41	6.0		1040400	22	2.1	
	1,7-Phe	502500	24	4.8	4.7 ± 0.5	963600	12	1.2	1.6 ± 0.6
		397500	19	4.8		962400	11	1.1	
		622000	33	5.3		1341000	21	1.6	
		332000	13	3.9		916900	24	2.6	

* Significantly different from the control group, $P < 0.05$.
** Significantly different from the control group, $P < 0.01$.

selection for *cII* mutants was performed according to the method of Jakubczak et al. [24] with slight modification as previously reported [14]. Briefly, the phage solution was absorbed to *E. coli* G1225 (*hfl*$^-$) at room temperature for 20–30 min. For titration, an appropriately diluted phage-*E. coli* solution was mixed with LB top agar (containing 10 mM $MgSO_4$), plated onto dishes containing bottom agar, and incubated for 24 h at 37 °C. The remaining phage-*E. coli* solution was mixed with LB top agar and plated onto dishes con-